

## Emission spectra of a $\Lambda$ -type quantum-beat three-level atom

M. M. Ashraf

*Department of Physics, Quaid-I-Azam University, Islamabad 45320, Pakistan*

(Received 6 July 1993; revised manuscript received 30 August 1993)

The emission spectra of a  $\Lambda$ -type quantum-beat three-level atomic system in a cavity is investigated. Our results suggest that the atom cannot interact with a single-mode squeezed vacuum. A variety of field inputs exhibit nonclassical effects, including the vacuum Rabi splitting and quantum beats, only for low field intensities. In the case of a coherent field input, sidebands appear whose widths are governed by the input field statistics. Off-resonant spectra exhibit transitions from predominantly spontaneous to predominantly stimulated emission.

PACS number(s): 42.50.Dv

### I. INTRODUCTION

In recent years, much interest has been focused on quantum dynamics of nonlinear systems. In this respect the nonlinear effects of a cavity-bound atom have received considerable attention. The radiation-matter interaction does influence the characteristics of the light emitted from it. Several studies [1-6] of the emission spectrum of the cavity-bound atom have led to the discovery of nonclassical phenomena, including vacuum Rabi splitting [1].

The  $\Lambda$ -type three-level system leading to a quantum-beat laser has novel properties [7]: it can lase without inversion, invert without lasing, and under certain physical conditions it can be reduced to a standard Jaynes-Cummings model [8]. The quantum-beat technique can be extended to systems with several closely spaced transitions. The time-varying signal becomes more complicated, but if the level spacings are larger than or equal to the damping coefficients of the levels [i.e.,  $(E_2 - E_1) \geq (\gamma_1 + \gamma_2)$ ], the spectrum can be obtained readily from the Fourier transform of the time-varying signal. The system is prepared in a coherent superposition of these states. The technique is most useful for finding small level splitting, so that the signal can be accurately measured using a conventional transient detection system. Both the time-varying signal and its Fourier spectrum can be directly displayed on the oscilloscope [9].

With this information in mind, we formulate the system of a single  $\Lambda$ -type three-level atom interacting with a single-mode electromagnetic field in an ideal (zero-loss) cavity in Sec. II. The spectrum of the emitted radiation, examined by a realistic spectrometer of bandwidth  $\Gamma$ , which is inside the cavity, is calculated in Sec. III followed by discussions in Sec. IV. Finally, a brief conclusion is presented in Sec. V.

### II. THE MODEL WITH FIELD AND ATOM STATES

The system under consideration is a  $\Lambda$ -configuration three-level atom (one upper and two lower levels) in-

teracting with a single mode field, as shown in Fig. 1. Initially, the atom is pumped into a coherent superposition of two lower states. In the so-called rotating-wave approximation the Hamiltonian can be given as

$$H = \omega(a^\dagger a + \frac{1}{2}) + \sum_{j=1}^3 \omega_j |j\rangle \langle j| + \lambda [a|3\rangle \langle \langle 1| + \langle 2| \rangle + a^\dagger (|1\rangle + |2\rangle) \langle 3|]. \quad (1)$$

Here  $a$  and  $a^\dagger$  are the annihilation and creation operators of the cavity field,  $\omega$  and  $\omega_j$  are the cavity field and the  $j$ th state atomic frequencies, respectively,  $\lambda$  is atom-field coupling constant, and for simplicity we use  $\hbar=1$ . We also assume that transitions from  $|3\rangle$  to  $|2\rangle$  and  $|3\rangle$  to  $|1\rangle$  are allowed and all other intermediate transitions are forbidden.

In order to simplify the system, we first define the following ket-bra operators

$$S^\dagger = \frac{1}{\sqrt{2}} |3\rangle \langle \langle 1| + \langle 2| \rangle, \quad (1a)$$

$$S = \frac{1}{\sqrt{2}} (|1\rangle + |2\rangle) \langle 3|, \quad (1b)$$

$$S_z = \frac{1}{2} [|3\rangle \langle 3| - \frac{1}{2} (|1\rangle + |2\rangle) \langle \langle 1| + \langle 2| \rangle], \quad (1c)$$

which satisfy the  $su(2)$  algebra, i.e.,

$$[S^\dagger, S] = 2S_z, \quad [S_z, S^\dagger] = S^\dagger, \quad [S_z, S] = -S. \quad (2)$$

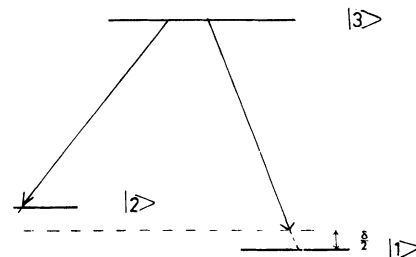


FIG. 1. Schematic diagram of a  $\Lambda$ -type quantum-beat three-level atomic system. The transitions  $|3\rangle$  to  $|1\rangle$  and  $|3\rangle$  to  $|2\rangle$  are dipole allowed.

By means of Eqs. (1a)–(1c), the Hamiltonian of Eq. (1) can be recast in the form

$$H = H_0 + H_I + H' + H'', \quad (3)$$

where

$$H_0 = \omega(a^\dagger a + \frac{1}{2}) + \omega_0 S_z, \quad H_I = \sqrt{2}(S^\dagger a + a^\dagger S),$$

$$H' = \frac{1}{4}\omega_0(|1\rangle - |2\rangle)(\langle 2| - \langle 1|),$$

$$H'' = \frac{1}{2}\delta(|2\rangle\langle 2| - |1\rangle\langle 1|).$$

Here  $\omega_0 = \omega_3 - (\omega_1 - \frac{1}{2}\delta)$ ,  $\delta = \omega_2 - \omega_1$ , and  $\omega_j$  ( $j=1,2,3$ ) is the atomic level frequency. Since we have assumed levels  $|1\rangle$  and  $|2\rangle$  to be almost degenerate, it is reasonable to consider that the populations in  $|1\rangle$  and  $|2\rangle$  are approximately equal. Hence  $H''$  can be neglected in comparison with the other terms in Eq. (3).

Notice that  $[H', S] = [H', S^\dagger] = [H', S_z] = 0$ . Thus we are able to apply the unitary transformation  $Q = \exp(iH't)$  to the state function  $\psi$  and get

$$\psi \rightarrow Q\psi = \psi', \quad i\frac{\partial\psi'}{\partial t} = \bar{H}\psi', \quad (4)$$

where

$$\begin{aligned} \bar{H} &= QHQ + iQQ^\dagger \\ &= \omega(a^\dagger a + \frac{1}{2}) + \omega_0 S_z + \sqrt{2}\lambda(a^\dagger S + S^\dagger a). \end{aligned} \quad (5)$$

This is a simplified form of the Hamiltonian of Eq. (1) and describes a  $\Lambda$ -type three-level system with the two lower levels almost degenerate and equally populated. It should be noted here that the  $S$  operators are quite different from the conventional Pauli operators. In fact we can rewrite Eqs. (1a)–(1c) in matrix representation as

$$S^\dagger = \frac{1}{\sqrt{2}} \begin{pmatrix} 0 & 1 & 1 \\ 0 & 0 & 0 \\ 0 & 0 & 0 \end{pmatrix},$$

$$S = \frac{1}{\sqrt{2}} \begin{pmatrix} 0 & 0 & 0 \\ 1 & 0 & 0 \\ 1 & 0 & 0 \end{pmatrix},$$

$$S_z = \frac{1}{2} \begin{pmatrix} 1 & 0 & 0 \\ 0 & -\frac{1}{2} & -\frac{1}{2} \\ 0 & -\frac{1}{2} & -\frac{1}{2} \end{pmatrix},$$

by means of the vectors

$$|1\rangle = \begin{pmatrix} 0 \\ 0 \\ 1 \end{pmatrix}, \quad |2\rangle = \begin{pmatrix} 0 \\ 1 \\ 0 \end{pmatrix}, \quad |3\rangle = \begin{pmatrix} 1 \\ 0 \\ 0 \end{pmatrix}. \quad (6)$$

In order to obtain the time evolution of the system, we can split the Hamiltonian into two parts,  $\bar{H} = N + C$ , where

$$N = \omega(a^\dagger a + \frac{1}{2}) + \omega_0 S_z, \quad (7a)$$

$$C = \Delta S_z + \sqrt{2}\lambda(a^\dagger S + aS^\dagger), \quad (7b)$$

with  $\Delta = \omega_0 - \omega$ . It can be proved easily that both  $N$  and  $C$  are constants of the motion, i.e.,  $[\bar{H}, N] = [\bar{H}, C] = [C, N] = 0$ . It then follows that the time evolution operator is

$$U(t, 0) = e^{-i\bar{H}t} = e^{-iNt} e^{-iCt}. \quad (8)$$

Using the matrix representation of the  $S$  operators one obtains

$$U(t, 0) = e^{-i\omega(a^\dagger a + 1/2)t} \begin{pmatrix} \alpha e^{-i\omega_0 t/2} & \beta e^{-i\omega_0 t/2} & \beta e^{-i\omega_0 t/2} \\ \mu e^{i\omega_0 t/2} & \frac{1}{2}(\alpha' e^{i\omega_0 t/2} + 1) & \frac{1}{2}(\alpha' e^{i\omega_0 t/2} - 1) \\ \mu e^{i\omega_0 t/2} & \frac{1}{2}(\alpha' e^{i\omega_0 t/2} - 1) & \frac{1}{2}(\alpha' e^{i\omega_0 t/2} + 1) \end{pmatrix}, \quad (9)$$

with

$$\alpha = \cos Bt - i\frac{\Delta}{2} \frac{\sin Bt}{B},$$

$$\alpha' = \cos B't + i\frac{\Delta}{2} \frac{\sin B't}{B'},$$

$$\beta = -i\lambda a \frac{\sin B't}{B'},$$

$$\mu = -i\lambda a^\dagger \frac{\sin Bt}{B},$$

$$B = \left[ \frac{\Delta^2}{4} + 2\lambda^2 a a^\dagger \right]^{1/2},$$

$$B' = \left[ \frac{\Delta^2}{4} + 2\lambda^2 a^\dagger a \right]^{1/2}.$$

In the next section we shall use the above formalism to calculate the emission spectrum of the system.

### III. EMISSION SPECTRUM OF A QUANTUM-BEAT THREE-LEVEL SYSTEM

The physical spectrum  $\underline{S}(\nu)$  of radiation emitted by a cavity-bound atom is given by the expression [10]

$$\begin{aligned} \underline{S}(\nu) &= 2\Gamma \int_0^T dt_1 \int_0^T dt_2 \exp[-(\Gamma - i\nu)(T - t_1) \\ &\quad - (\Gamma + i\nu)(T - t_2)] \\ &\quad \times \langle \psi_{AF} | S^\dagger(t_1) S(t_2) | \psi_{AF} \rangle, \end{aligned} \quad (11)$$

where  $T$  is the interaction time (fixed at  $20/\lambda$  for the present case) and  $\Gamma$  is the bandwidth of the filter.  $|\psi_{AF}\rangle$  is the initial state of the system. If the atom is in the top

state  $|3\rangle$  and the field is in the superposition of the number states, i.e.,

$$|\psi_{AF}\rangle = \sum_n C_n |3;n\rangle, \quad (12)$$

then one can easily find

$$S(t)|3;n\rangle = U^\dagger(t,0)S(0)U(t,0) \begin{pmatrix} 1 \\ 0 \\ 0 \end{pmatrix} |n\rangle, \quad (13)$$

where  $S(0)$  and  $U(t)$  are given in Eqs. (6) and (9), respectively. Now it is quite straightforward to calculate the two-time correlation function

$$\begin{aligned} & \langle \psi_{AF} | S^\dagger(t_1) S(t_2) | \psi_{AF} \rangle \\ &= e^{-i\omega(t_2-t_1)} \sum_n \rho_{nn} f_n^*(t_1) f_n(t_2) f_{n-1}(t_2-t_1), \end{aligned} \quad (14)$$

where

$$\begin{aligned} f_n(t) &= \frac{1}{2} \left[ \left[ 1 + \frac{\Delta}{2\Omega} \right] e^{-i\Omega t} + \left[ 1 - \frac{\Delta}{2\Omega} \right] e^{i\Omega t} \right], \\ \Omega &= \Omega(n) = \left[ \frac{\Delta^2}{4} + 2\lambda^2(n+1) \right]^{1/2}, \\ \rho_{nn'} &= C_n^* C_{n'}. \end{aligned} \quad (15)$$

Substituting Eqs. (14) and (15) into Eq. (11) and carrying out the integration over the interaction time, we get the following expression for the emission spectrum:

$$\mathcal{S}(\nu, T) = \sum_n \rho_{nn} \mathcal{T}_n(\nu, T), \quad (16)$$

with the spectral function

$$\begin{aligned} \mathcal{T}_n(\nu, T) &= \frac{\Gamma}{4} [ |F_n^+(\Omega, \Omega', T) + F_n^+(-\Omega, \Omega', T)|^2 \\ &\quad + |F_n^+(-\Omega, -\Omega', T) + F_n^+(\Omega, -\Omega', T)|^2 ], \end{aligned} \quad (17)$$

with

$$\begin{aligned} F_n^+(\Omega, \Omega', T) &= \left[ 1 + \frac{\Delta}{2\Omega} \right] \left[ 1 + \frac{\Delta}{2\Omega'} \right]^{1/2} \\ &\quad \times \frac{e^{i(\omega-\nu+\Omega+\Omega')T} - e^{-\Gamma T}}{\Gamma + i(\omega-\nu+\Omega+\Omega')}, \end{aligned} \quad (18)$$

and

$$\Omega' = \left[ \frac{\Delta^2}{4} + 2\lambda^2 n \right]^{1/2}. \quad (19)$$

In the next section we shall give the results based on Eqs. (14)–(19).

#### IV. RESULTS AND DISCUSSIONS

Section IV A gives the results and discussions of the calculations when the input field is assumed to be in a pure number state. Results of the case when the field is in a superposition of number states are discussed in Sec. IV B.

##### A. Initial field in pure number states

Let us first discuss the emission spectra for pure number states, which are the  $|n\rangle$  basis states shown in Fig. 2. Because of the four sign combinations in Eqs. (16)–(19), one expects to see four peaks. In general they occur at  $\nu-\omega = \pm(\Omega+\Omega')$  and  $\nu-\omega = \pm(\Omega-\Omega')$ . However, in the vacuum state  $|n=0\rangle$  for  $\Delta=0$ , the resonance case, we obtain only two peaks, symmetrically located around  $\nu-\omega = \pm\sqrt{2}\lambda$ , which is just the vacuum Rabi splitting [1]. For any other initial number state  $|n\rangle$ ,  $n \neq 0$ , the spectrum shows either three or four peaks. For  $n \gg 1$  and for a finite resolution spectrometer the central two peaks start coalescing and the outer ones recede away from each other, leading to a three-peak structure. In this way, for large photon numbers one obtains the basic shape of the semiclassical three-peak spectrum of the resonance fluorescence [11].

For the nonresonant case ( $\Delta \neq 0$ ), when the initial field is in the vacuum state the inner two peaks are located at

$$\nu-\omega = \pm \left[ \left[ \frac{\Delta^2}{4} + 2\lambda^2 \right]^{1/2} - \frac{\Delta}{2} \right]$$

and the outer ones at

$$\nu-\omega = \pm \left[ \left[ \frac{\Delta^2}{4} + 2\lambda^2 \right]^{1/2} + \frac{\Delta}{2} \right].$$

If  $\Delta \gg \lambda$ , the inner peaks occur at  $\nu-\omega = \pm 2\lambda^2/\Delta$ , i.e., the vacuum field Rabi splitting becomes much less noticeable compared to the resonant case. The central two-peak structure stands out clearly for large initial photon numbers in the case of  $\lambda n \gg \Delta$ . These peaks now occur at

$$\nu-\omega = \pm \lambda \{ [2(n+1)]^{1/2} - (2n)^{1/2} \}.$$

##### B. Initial field in superposition of number states

For the study of nonclassical effects exhibited, if any, by the system, we now focus our attention on Fig. 3. Since the photon-number distribution plays a decisive

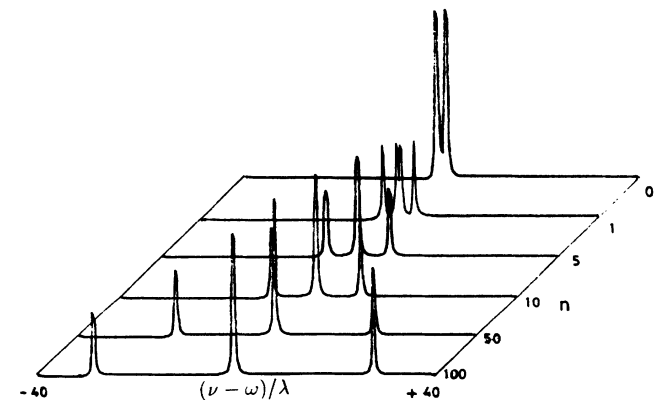


FIG. 2. The number state spectra  $\mathcal{T}_n(\nu)$  as a function of  $(\nu-\omega)/\lambda$ , a dimensionless quantity, with interaction time  $T=20/\lambda$ , resolution of the spectrometer  $\Gamma=0.2\lambda$ , and  $\Delta=0$ .

role in the formation of the spectra, the comparison is made for the same number of  $\bar{n}$ .

In the case of a squeezed vacuum input [Fig. 3(a)],  $\rho_{2n,2n}$  is peaked at  $n=0$  ( $\rho_{2n+1,2n+1}=0$ ) and falls off sharply as we move away from this value. The photon-number variance  $(\Delta n)^2$  is proportional to  $2\bar{n}(\bar{n}+1)$  [3], where  $\bar{n}=\sinh^2 r$  and grows with squeezing parameter  $r$ . Referring to Eqs. (16)–(19) ( $n$  is replaced by  $2n$  in these equations only for this case), it is clear that Rabi peaks dominate the spectrum for small  $\bar{n}$ . With the increase in

$\bar{n}$  more and more photon-number-state spectra have to be included in the sum. The small peaks due to quantum beats emerge and modify the wings. At larger  $\bar{n}$ , the Rabi splitting peaks are suppressed by quantum beats and at  $\bar{n} \geq 10$  these effects start reducing and we move towards a single-peak spectrum. Here the Rabi peaks survive for larger  $\bar{n}$  values than they do for thermal input. This is due to the larger relative weight of the vacuum state in the squeezed vacuum field distribution. For the thermal field distribution [Fig. 3(b)]  $(\Delta n)^2$  is proportional to  $\bar{n}(\bar{n}+1)$  and decays relatively slowly. That is why the transition from a double-peak to a single-peak spectrum starts much earlier. Since both distributions are similar at large  $n$  (even though their slopes are different) and their behavior is more or less similar, they have no peaks other than at  $n=0$  and no coherent sidebands emerge for either the squeezed vacuum or the thermal case.

The situation is quite different for the coherent field input, shown in Fig. 3(c). The photon distribution  $\rho_{nn}$  is peaked at  $\bar{n}$ , with a width  $\sqrt{\bar{n}}$  (as opposed to of the order of  $\bar{n}$  for squeezed vacuum and thermal cases). The spectrum is still dominated by the Rabi peaks for small  $\bar{n}$  along with modified wings due to quantum beats. When  $\bar{n}$  is increased, the relative weight of the vacuum state diminishes rapidly and additional peaks appear on both sides of the structure. The coherent sidebands start emerging. These sidebands are suppressed by quantum beats and from  $\bar{n} \geq 5$  they not only move away from the central peak position but also broaden. Compared with the previous cases, quantum beats induce a more rapid transition from a double-peak to a single-peak structure with increasing  $\bar{n}$ .

The width of the central peak is determined only by the resolution of the detector. This means that even though the spectra in Fig. 3 look “classical,” they really are not. The usual Mollow spectrum for an atom in free space [11] contains precise values for the ratio of the heights of the peaks which are broadened by the level lifetime (spontaneous emission). In this case the different ratios of heights and subnatural linewidths arise from the suppression of spontaneous emission in all of the other field modes. This spontaneous emission emerges due to the vacuum fluctuations. The detector sees only the filtered version of the single-mode cavity field and is set at frequency  $\nu$  [10].

For the nonresonant case  $\Delta=5\lambda$ , shown in Fig. 4, the spectra of Fig. 3 are modified to a structure containing asymmetric peaks. At low field intensities, vacuum fluctuations dominate the spectra and the spontaneous emission peaks are mostly centered at  $\nu-\omega=5\lambda$ ; however, as  $\bar{n}$  increases, the effect of the vacuum fluctuations decreases and the stimulated emission peak at  $\nu=\omega$  becomes dominant. This transition from predominantly spontaneous to predominantly stimulated emission can be seen in Figs. 4(a)–4(c). However, in the case of the squeezed vacuum input [Fig. 4(a)], the spectrum shows more structure around the fluorescence peak and survives for larger  $\bar{n}$ , which is missing in the thermal case. In the case of the coherent input [Fig. 4(c)], the dominating fluorescence peak at low  $\bar{n}$  does not disappear for larger  $\bar{n}$ . It shifts towards higher frequencies and eventually

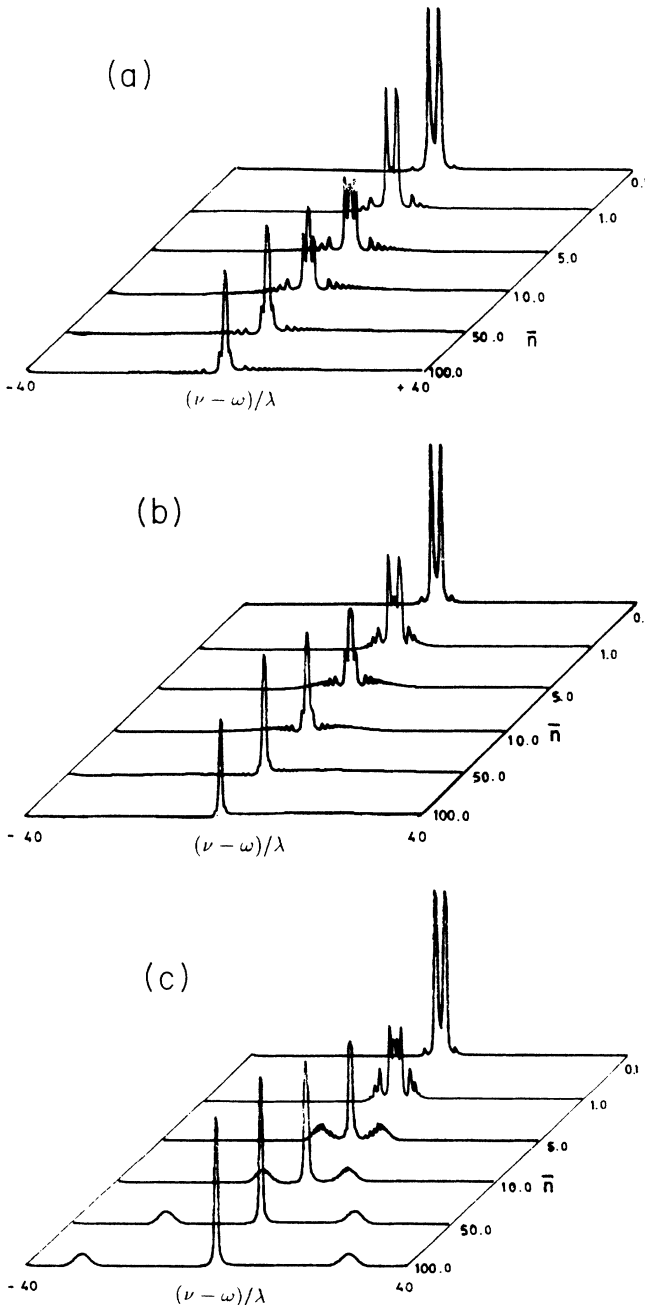


FIG. 3. Emission spectra for (a) a squeezed vacuum input, (b) a thermal input, and (c) a coherent input with the same parameters as in Fig. 2.

turns into a sideband at a distance  $2[\Delta^2/4 + 2\lambda^2\bar{n}]^{1/2}$  away from the cavity frequency  $\omega$ .

### V. CONCLUSION

We have analyzed the emission spectra of a  $\Lambda$ -type quantum-beat three-level atomic system in a cavity with the two lower levels almost degenerate and equally populated and conclude that the nonclassical effects arise from the suppression of spontaneous emission in all other field modes. They are dependent on the resolution of the detector. The spectrum differs from the classical Mollow spectrum for an atom in free space in terms of its variation in the ratio of peak heights and subnatural linewidths. There is a remarkable similarity in the spectra of the squeezed vacuum and those of the thermal in-

puts, as the former is insensitive to the relative phase between the atomic dipole and the squeezed field, in contrast to the results in Refs. [12,13]. Our results suggest that atom cannot interact with a single-mode squeezed vacuum. In two-photon transition the photon pair is emitted and absorbed simultaneously. Interestingly, the vacuum Rabi splitting is more prominent for the squeezed vacuum input field than for the thermal input field with comparable photon numbers. This is due to the fact that the vacuum state has a larger relative weight in the makeup of a squeezed vacuum. Eventually, it is washed out for large field intensities, as can be seen, from number state spectra of Fig. 2. The coherent sidebands, however, stand for all  $\bar{n}$  values, but vary their widths with input field intensities even though they are suppressed by quantum beats.

A comparison between the on-resonance and off-

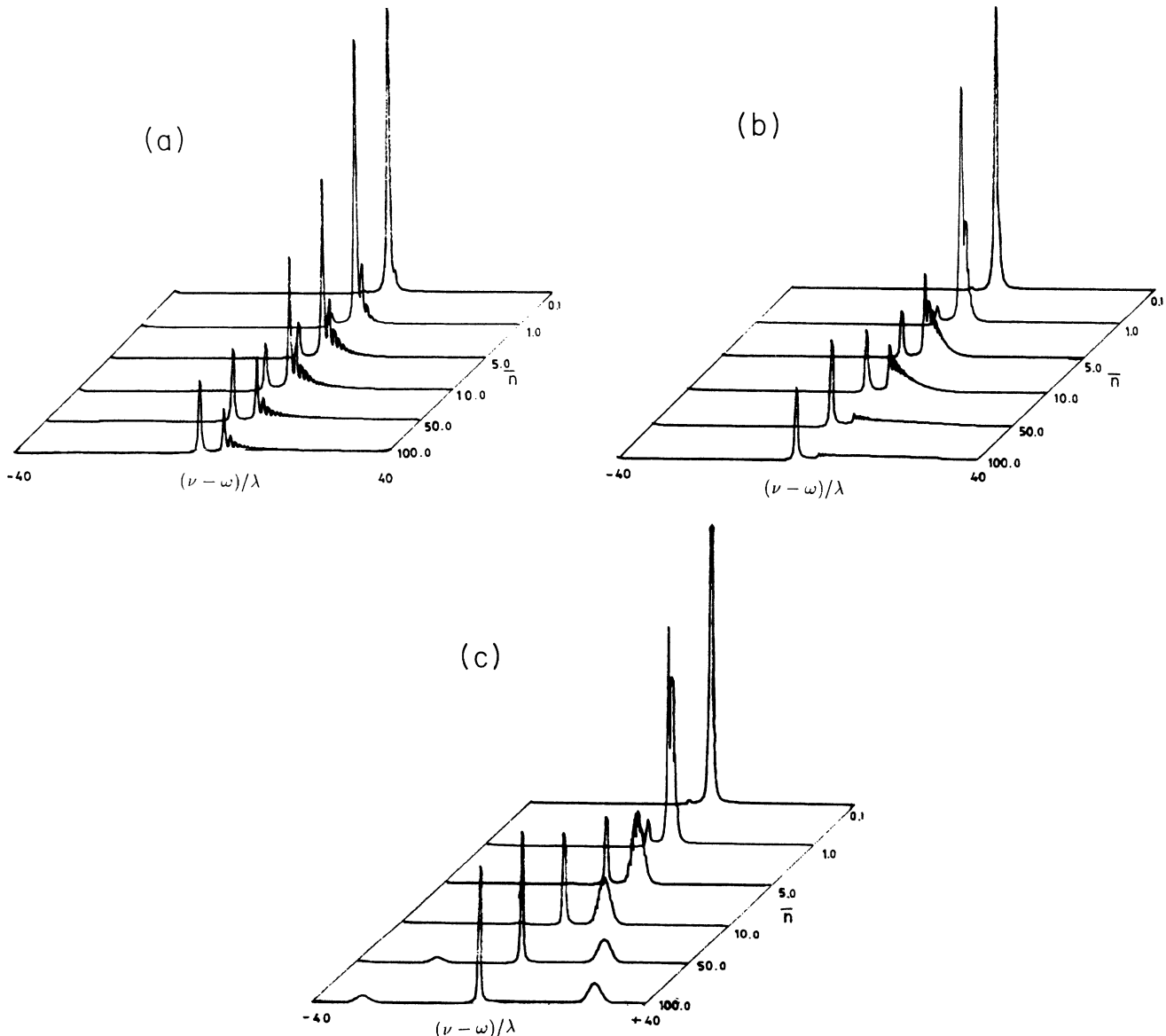


FIG. 4. Emission spectra for (a) a squeezed vacuum input, (b) a thermal input, and (c) a coherent input for  $\Delta = 5\lambda$  with the same parameters as in Fig. 2.

resonance excitations reveals that the quantum-beat effects and coherent sidebands are more prominent in the former case. But in the latter case, a transition from predominantly spontaneous to predominantly stimulated emission as we move from low  $\bar{n}$  to high  $\bar{n}$  is quite evident, and the vacuum Rabi splitting is much less transparent. Recently, Field [14] has observed vacuum Rabi splitting with population-trapping techniques in the same model. He has stated a condition for lasing without inversion without any externally injected coherent field.

The model under discussion could also lead to a correlated emission laser if the transitions are made via two photons. Detailed investigations are being carried out and will be presented in a future paper.

#### ACKNOWLEDGMENT

The author would like to acknowledge Prof. Dr. A. H. Nayyar for useful discussions.

- 
- [1] N. B. Narozheny, J. J. Sanchez-Mondragon, and J. H. Eberly, *Phys. Rev. A* **23**, 236 (1981).
  - [2] J. J. Sanchez-Mondragon, N. B. Narozheny, and J. H. Eberly, *Phys. Rev. Lett.* **51**, 550 (1983).
  - [3] J. Gea-Banacloche, R. R. Schlicher, and M. S. Zubairy, *Phys. Rev. A* **38**, 3514 (1988); G. S. Agrawal, *Phys. Rev. Lett.* **67**, 980 (1991).
  - [4] V. Buzek and I. Jex, *Quantum Opt.* **2**, 147 (1990).
  - [5] V. Buzek, I. Jex, and M. Brisudova, *Int. J. Mod. Phys. B* **5**, 797 (1977).
  - [6] M. M. Ashraf and M. S. K. Razmi, *Phys. Rev. A* **45**, 8121 (1992).
  - [7] M. O. Scully, S. Y. Zhu, and A. Gavrielides, *Phys. Rev. Lett.* **62**, 2813 (1989).
  - [8] Hong-bin Hung and Hong-Yi Fan, *Phys. Lett. A* **159**, 323 (1991).
  - [9] Y. R. Shen, *The Non-Linear Optics* (Wiley, New York, 1984), p. 216; S. Haroche, J. A. Pasner, and A. L. Schawlow, *Phys. Rev. Lett.* **30**, 948 (1973).
  - [10] J. H. Eberly and K. Wodkiewicz, *J. Opt. Soc. Am.* **67**, 1252 (1977).
  - [11] B. R. Mollow, *Phys. Rev.* **188**, 1969 (1969); *Phys. Rev. A* **5**, 1522 (1972).
  - [12] C. W. Gardiner, *Phys. Rev. Lett.* **56**, 1917 (1986).
  - [13] H. J. Carmichael, A. S. Lane, and W. F. Walls, *Phys. Rev. Lett.* **58**, 2539 (1987).
  - [14] J. E. Field, *Phys. Rev. A* **47**, 5064 (1993); **48**, 2486 (1993).